A Dynamically Computed Convective Time Scale for the Kain–Fritsch Convective Parameterization Scheme

O. RUSSELL BULLOCK JR., KIRAN ALAPATY, AND JEROLD A. HERWEHE

National Exposure Research Laboratory, U.S. Environmental Protection Agency, Research Triangle Park, North Carolina

JOHN S. KAIN

National Severe Storms Laboratory, National Oceanic and Atmospheric Administration, Norman, Oklahoma

(Manuscript received 31 July 2014, in final form 29 January 2015)

ABSTRACT

Many convective parameterization schemes define a convective adjustment time scale τ as the time allowed for dissipation of convective available potential energy (CAPE). The Kain–Fritsch scheme defines τ based on an estimate of the advective time period for deep convective clouds within a grid cell, with limits of 1800 and 3600 s, based on practical cloud-lifetime considerations. In simulations from the Weather Research and Forecasting (WRF) Model using 12-km grid spacing, the value of τ often defaults to the lower limit, resulting in relatively rapid thermodynamics adjustments and high precipitation rates. Herein, a new computation for τ in the Kain–Fritsch scheme is implemented based on the depth of the buoyant layer and the convective velocity scale. This new τ formulation is applied using 12- and 36-km model grid spacing in conjunction with a previous modification that takes into account the radiation effects of parameterized convective clouds. The dynamically computed convective adjustment time scale is shown to reduce the precipitation bias by approximately 15% while also providing improved simulations of inland rainfall from tropical storms.

1. Introduction

Previous applications of the Weather Research and Forecasting (WRF) Model for dynamical downscaling, as described in Otte et al. (2012), Bowden et al. (2012, 2013), and Bullock et al. (2014), have shown a general tendency for simulations to produce too much precipitation, especially for the warm seasons. To treat parameterized convection in a more realistic manner, Alapaty et al. (2012) modified the Kain–Fritsch convective parameterization scheme (CPS) and the Rapid Radiative Transfer Model for GCMs (RRTMG) to simulate the radiative effects of subgrid-scale convective clouds. This resulted in a significant decrease in simulated convective precipitation and reduced the positive bias in total precipitation in WRF simulations using 36-km grid spacing (Herwehe et al. 2014). However, when these subgrid radiation treatments were applied in this study using 12-km grid spacing, a considerable positive bias remained. The excess convective precipitation appeared to be worse at finer resolution, so the Kain–Fritsch parameterization was examined with a special focus on scale-sensitive formulations. One such formulation was found having to do with the convective adjustment time scale.

The convective adjustment time scale τ, also called the relaxation time scale, is the hypothetical time required for deep moist convective overturning to adjust thermodynamic profiles to a quasi-equilibrium or neutral state. As discussed by Frank (1983), the factors that modulate both the time and space scales of convective adjustment are complicated, dependent on local dynamical constraints, and not completely understood. In numerical models, convective parameterizations are generally applied in individual grid columns, in effect constraining the spatial scale of adjustment for a given model configuration, but there is no universal agreement on how to define an appropriate corresponding time scale. Early convective adjustment schemes acted instantaneously—temperature and water vapor adjustments were applied in a single model time step (e.g.,

Corresponding author address: O. Russell Bullock Jr., EPA/ORD/NERL/AMAD, 109 T. W. Alexander Dr., MD-E243-01, Research Triangle Park, NC 27711.
E-mail: bullock.russell@epa.gov

DOI: 10.1175/MWR-D-14-00251.1

Manabe et al. 1965)—motivated by the fundamental objective of not allowing potentially unstable layers to become saturated in a model. Betts (1986) proposed allowing this time period to encompass many model time steps while still keeping it small enough (and thus the adjustment rate large enough) to maintain subsaturation in potentially unstable layers. Similarly, other studies such as those of Kuo (1974) and Frank and Cohen (1987) tied the adjustment rate to the rate of local moisture and mass convergence, respectively.

Fritsch and Chappell (1980) focused on the idea that moist convection stabilizes the local environment by replacing unstable air at low levels with less unstable air from above, through the action of convective downdrafts. They assumed that this process proceeds systematically as convective updraft–downdraft couplets move over an area, ingesting low-level unstable air and leaving more stable air in their wake. Accordingly, they linked the convective adjustment time scale to the advective time scale of clouds in a grid element. This concept was carried over to the Kain–Fritsch (Kain and Fritsch 1993) parameterization. Specifically, in this scheme τ was calculated by dividing the horizontal grid length by the vector average of the wind speed at cloud base and the 500-hPa pressure level. Based on early testing and observations of typical cloud lifetimes, τ was restricted to a maximum value of 3600 s and a minimum value of 1800 s. While this concept works fairly well for coarse grid resolutions, it leads to a shorter adjustment time scale at higher resolutions. This invigorates parameterized convection in fine-grid modeling where at least some of the convective energy might be resolvable.

None of these approaches for τ estimation has been universally accepted by the broader community, yet numerous studies have indicated that a variety of simulations are very sensitive to specified values of τ (e.g., Emanuel et al. 1994; Lin et al. 2000; Alapaty et al. 1994a, 1994b). Consequently, the magnitude of τ is often chosen on the basis of trial and error. For example, in a high-resolution regional modeling study, Done et al. (2006) concluded that usage of a large τ (~24 h) practically eliminated subgrid-scale precipitation while small τ (~600 s) resulted in a predominant subgrid-scale precipitation pattern. In many general circulation models, τ ranges from about one to a few hours (e.g., Zhang and McFarlane 1995; Collins et al. 2006; Wilcox and Donner 2007). In a high-resolution global climate simulation study, Bacmeister et al. (2007) found that usage of larger τ led to marked improvements in hurricane spinup time and intensity. Lucas et al. (2010) have shown that among other uncertain parameters, τ was found to be one of the most influential specified parameters in their global climate simulations. Using the Community Atmosphere Model, Liu et al. (2007) studied the climate response to various constant values of τ and found that no single value of this parameter produced optimal results for all aspects of climate. Results obtained from these and many other climate modeling studies demonstrate that specification of a particular τ value is problematic. This highlights the need for a spatially and temporally varying value of τ.

One way of doing this was tested by Bechtold et al. (2008). They made τ a function of simulated cloud depth, updraft vertical velocity averaged over the cloud layer, and a factor dependent on global model spectral resolution. They obtained probability density functions from several global forecasts with different spectral resolutions indicating that τ can be as small as 600 s and as high as 3 h. To improve the treatment of the relaxation time scale in the Kain–Fritsch convection scheme (Kain 2004) as it is employed in the WRF Model (Skamarock et al. 2008), we have developed a similar formulation for τ based on convective cloud depth and convective velocity scale and have applied that new formulation in WRF using 12-km grid spacing. The analysis presented here will deal primarily with the effects of our new τ formulation on precipitation bias, with a cursory examination of its effects on surface-level temperature, humidity, and wind speed.

2. Model and experiment design

The standard Kain–Fritsch CPS defines τ simply as the model grid spacing divided by the average of the wind speeds at the lifting condensation level (LCL) and the 500-hPa level. The value of τ is then limited to the range of 1800–3600 s. However, given the same wind conditions, this formulation tends to force the dissipation of CAPE more quickly with stronger updrafts for model applications using finer grid spacing. As the horizontal resolution of the model approaches the so-called gray scales where convection is at least partially resolved by model dynamics, we would expect to see the opposite effect where the CPS has less impact. For these reasons, we propose an alternate formulation for τ.

a. *Dynamic τ formulation*

Based on the previous work of Bechtold et al. (2008), we adopted a similar formulation for τ that omits a scaling factor dependent on model resolution and considers the effect of convective overturning throughout each grid column where convective updrafts may exist. Our dynamic formulation includes only the depth of the convective cloud divided by a convective cloud velocity scale w_c similar to that described by Grant and Lock (2004) based on BOMEX observations (Holland and

Rasmusson 1973) and large eddy simulation of shallow convection.

Our initial estimate for the convective adjustment time scale (s) is given by

$$\tau_0 = \frac{z_{\text{Eq.Lev.}} - z_{\text{LCL}}}{w_c}, \quad (1)$$

where $z_{\text{Eq.Lev.}}$ is the height (m) of the equilibrium level and z_{LCL} is the height (m) of the LCL, both of which are calculated as part of the Kain–Fritsch CPS and their difference is considered as the depth of the convective cloud. Equation (1) is analogous to the formulation suggested by Bechtold et al. (2008). The convective cloud velocity scale w_c (m s^{-1}) used here was suggested for shallow convective clouds (Grant and Lock 2004). Measurements necessary for calibrating the magnitude of the velocity scale for deep convective clouds do not exist, but a theoretical basis was documented by Emanuel and Bister (1996). A global constant parameter ϙ may be needed to make this formulation for w_c suitable for deep convection. We introduce such a constant ϙ, but set it to unity for these initial numerical simulations at 12-km grid spacing. The convective velocity scale is defined as

$$w_c = (\text{ϙ} \times m_b \times \text{ABE})^{1/3}, \quad (2)$$

where m_b is described by Grant and Lock (2004) as the cloud-base mass flux per unit density (m s^{-1}) and ABE is the available buoyant energy (m^2 s^{-2}), including entrainment, taken from the Kain–Fritsch CPS. Note that Grant and Lock (2004) only considered adiabatic buoyancy, so the convective velocity scale from Eq. (2) differs somewhat as a result of the consideration of entrainment. Equation (2) holds well for shallow convective clouds and can be used for deep convective clouds as well since the right-hand side of Eq. (2) is not too different from the cube root of the vertically integrated buoyancy flux over the cloud depth, as shown by Emanuel and Bister (1996) for undiluted buoyancy. Also, this term is similar to the cloud work function introduced by Arakawa and Schubert (1974), which is defined as kinetic energy generation per unit cloud-base mass flux, and, in the case of deep convective clouds, the product of ϙ and m_b is related to the mean updraft mass flux. For the model grid scale, cloud-base mass flux per unit density is calculated as

$$m_b = \frac{\text{VMT}_{\text{LCL}}}{(\Delta x)^2 \times \rho_{\text{LCL}}}, \quad (3)$$

where VMT_{LCL} is the vertical mass transfer rate (kg s^{-1}) within the updraft at the LCL that is required to consume at least 90% of the initial ABE, as determined by the Kain–Fritsch CPS; Δx is the horizontal grid spacing (m) for our WRF simulations; and ρ_{LCL} [atmospheric density (kg m^{-3}) at the LCL] is calculated from the local pressure and temperature (p_{LCL} and T_{LCL}, respectively, both available from the Kain–Fritsch CPS) using the ideal gas law. Since deep convective clouds are vertically resolved, their depth as well as the ABE estimations are determined on resolvable scales. Thus, our final formulation for τ is applicable at resolved scales representing the convective turnover time required to remove most of the ABE.

Once our initial estimate is calculated, the final value for τ is constrained to be within the range of $1800 \leq \tau \leq 18\,000$ s (0.5–5 h). The Kain–Fritsch CPS has a minimum cloud depth of about 4000 m to trigger deep convection. Our preliminary tests with 10-day simulations indicated that τ could be as low as 900 s for clouds less than 5000 m deep, while for clouds that are over 10 000 m deep in humid environments τ can be around 15 000 s. The lower limit of 1800 s was selected to maintain consistency with the original Kain–Fritsch formulation.

b. WRF Model configuration

Our dynamic τ formulation was initially tested in applications of WRF version 3.4.1 (using the Advanced Research WRF configuration) with 12-km grid spacing and a modeling domain covering the area shown in Fig. 1. We later repeated our testing regimen using 36-km grid spacing to see if the improvements we found were sensitive to the horizontal resolution. The model was configured three different ways for both horizontal resolutions, the first using the regular Kain–Fritsch CPS (case KF), the second using the modified Kain–Fritsch/RRTMG of Alapaty et al. (2012) to account for the radiative effects of parameterized convection (case RadKF), and the third using both the modified Kain–Fritsch/RRTMG and the new dynamic τ formulation (case RadTauKF). The simulations covered the 3-yr period from 0000 UTC 1 January 2005 to 0000 UTC 1 January 2008. All simulations used analysis nudging toward NCEP–DOE AMIP-II Reanalysis data (Kanamitsu et al. 2002) with nudging coefficients dependent upon the horizontal resolution. Stauffer and Seaman (1994) recommend weaker nudging at finer scales. Based on sensitivity tests in Bullock et al. (2014), the nudging coefficients used in this study for 12-km grid spacing were equal to 5×10^{-5} s^{-1} for the potential temperature and wind components and 5×10^{-6} s^{-1} for the water vapor mixing ratio. For 36-km grid spacing, these coefficients were a factor of 2 larger. This nudging

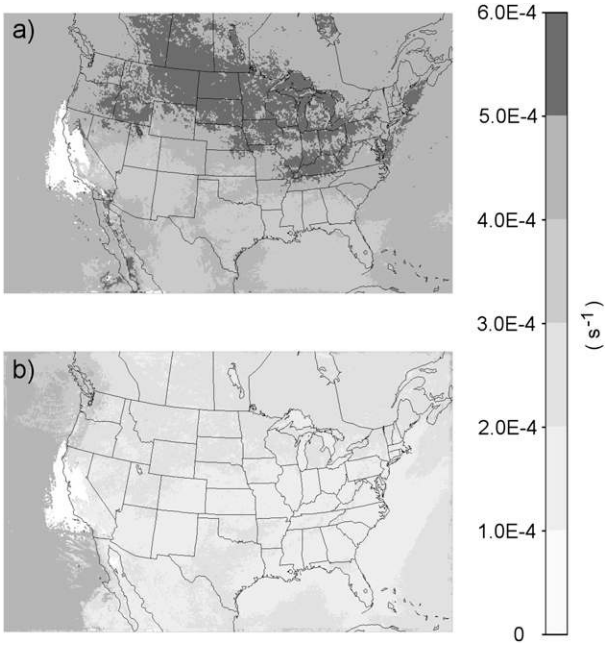

FIG. 1. Maps showing the average rate of CAPE dissipation ($1/\tau$) during July 2006 across the 480 × 300 array of 12-km grid cells of the WRF Model from (a) the standard Kain–Fritsch formulation and (b) the new dynamic τ formulation. White grid cells show where the convective parameterization was not required during the entire month.

toward a reference state, in this case toward a reanalysis field, certainly diminishes the sensitivity to changes in the convective parameterization. However, the motivation for this research was to improve dynamical downscaling methods, which rely on nudging. Also, the nudging coefficients used here are much smaller (weaker nudging) than the WRF default values, especially for water vapor mixing ratio, and are the values found to be optimum for 12-km dynamical downscaling as applied in Bullock et al. (2014) and applied for 36-km downscaling in Otte et al. (2012).

Initial and boundary conditions for all cases were obtained from previous WRF simulations using the standard Kain–Fritsch CPS over a slightly larger domain with 108- and 36-km nested grids. The parent 108- and 36-km simulations also used analysis nudging toward the NCEP–DOE AMIP-II Reanalysis data. In all cases, WRF was run using the same 34-layer configuration and 50-hPa model top used to evaluate the general approach to downscaling to 12-km grid spacing described in Bullock et al. (2014). Other WRF Model configuration options employed were also the same as in Bullock et al. (2014), namely the Yonsei University planetary boundary layer scheme (Hong et al. 2006), the Noah land surface model (Chen and Dudhia 2001), and the WRF single-moment 6-class microphysics scheme (Hong and Lim 2006).

3. Impact of the new formulation on the convective adjustment time scale

Figure 1 shows the effect of the dynamic τ formulation in slowing the dissipation of CAPE in our modeling with 12-km grid spacing. As a typical summertime example, the top map in Fig. 1 shows the July 2006 average rate of CAPE dissipation ($1/\tau$) from the standard Kain–Fritsch formulation (cases KF and RadKF) while the lower map shows the result from our dynamic τ formulation (case RadTauKF). In areas where lower-tropospheric winds have considerable velocity even during midsummer, the standard formulation produces τ values near the minimum limit of 1800 s and the monthly average rate of CAPE dissipation can exceed $5 \times 10^{-4}\,s^{-1}$. Most of the model domain in Fig. 1a shows an average CAPE dissipation rate of over $4 \times 10^{-4}\,s^{-1}$, including the area over the Pacific Ocean where shallow convection commonly occurs. The Kain–Fritsch CPS applies a predefined τ of 2400 s for shallow convection. Thus, the average CAPE dissipation rate in that area is 1/2400 or $4.1667 \times 10^{-4}\,s^{-1}$. When the dynamic τ formulation is applied (Fig. 1b), most of the model domain shows average CAPE dissipation rates of less than $3 \times 10^{-4}\,s^{-1}$ with some areas much lower because of the increased τ upper limit of 18 000 s versus 3600 s in the standard formulation. Again, shallow convection over the Pacific Ocean results in larger CAPE dissipation rates since the predefined τ value of 2400 s is also applied for shallow convection in our dynamic formulation.

a. *Effect on monthly average precipitation*

Figure 2 shows average monthly accumulated precipitation from 2005 through 2007 over the continental United States as indicated by the Parameter-Elevation Relationships on Independent Slopes Model (PRISM; Daly et al. 1994) compared to corresponding values simulated by all three WRF runs with 12-km grid spacing. Monthly average WRF and PRISM precipitation was calculated for all model grid cells over land using special scripts derived from the Atmospheric Model Evaluation Tool (AMET) described in Appel et al. (2011). A positive bias is evident in the control case KF, as was also shown by Bullock et al. (2014). The modified radiation treatment that accounts for the effect of subgrid-scale clouds reduced precipitation to a large degree, but still left a considerable positive bias. The new dynamic τ formulation (in addition to the modified radiation) provides further correction of that positive precipitation bias during the boreal spring

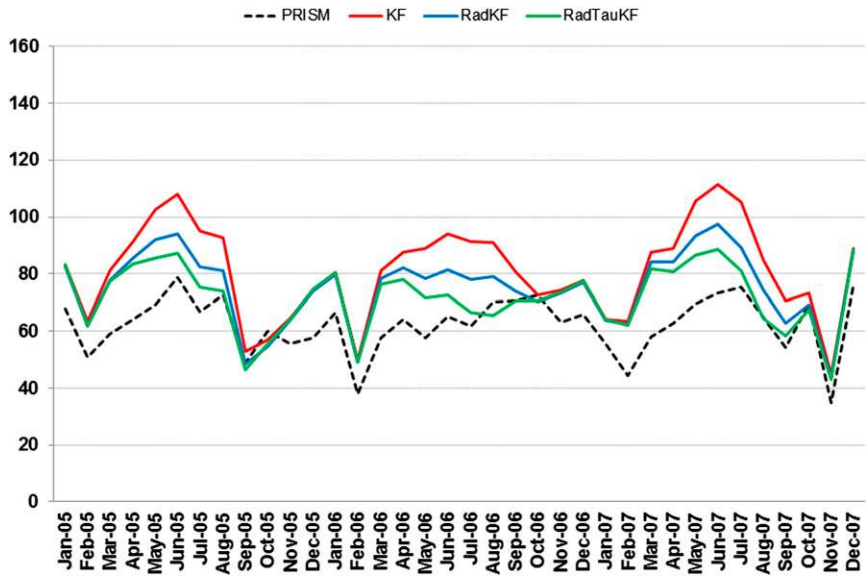

FIG. 2. Average monthly accumulated precipitation from WRF test cases using 12-km grid spacing vs data from PRISM.

and summer months when convection is known to produce a significant fraction of the total precipitation.

Over the entire 3-yr test period, WRF using the standard Kain–Fritsch CPS (case KF) resulted in an average precipitation bias of +30% relative to PRISM. When only the subgrid radiation effects were taken into account (case RadKF), this overall bias was reduced to +21%. With the addition of our dynamic τ formulation to the subgrid radiation treatment (case RadTauKF), the overall precipitation bias was reduced to +15% of the observed amount as represented by the PRISM analysis.

To investigate whether the improvements described above were robust and not limited to our choice of numerical settings for 12-km grid spacing, we repeated the testing regimen using a larger grid spacing and obtained

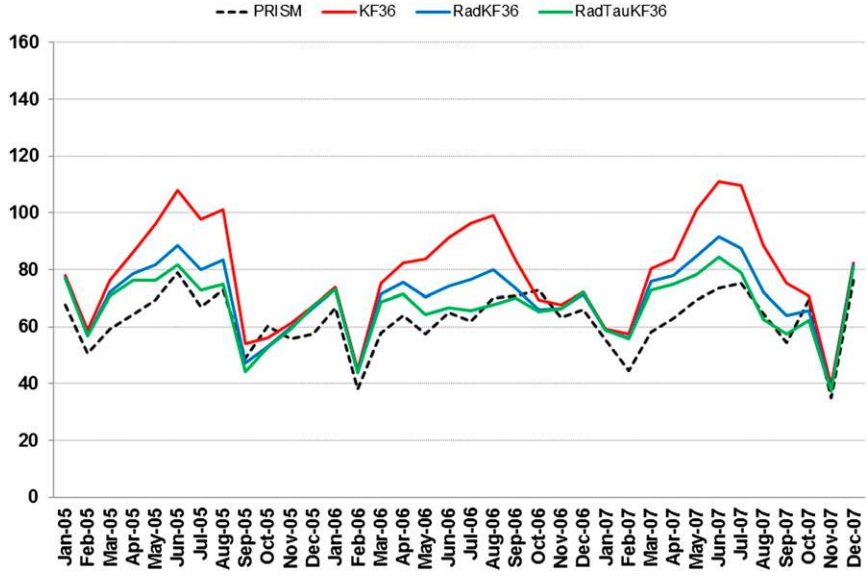

FIG. 3. As in Fig. 2, but for 36-km grid spacing.

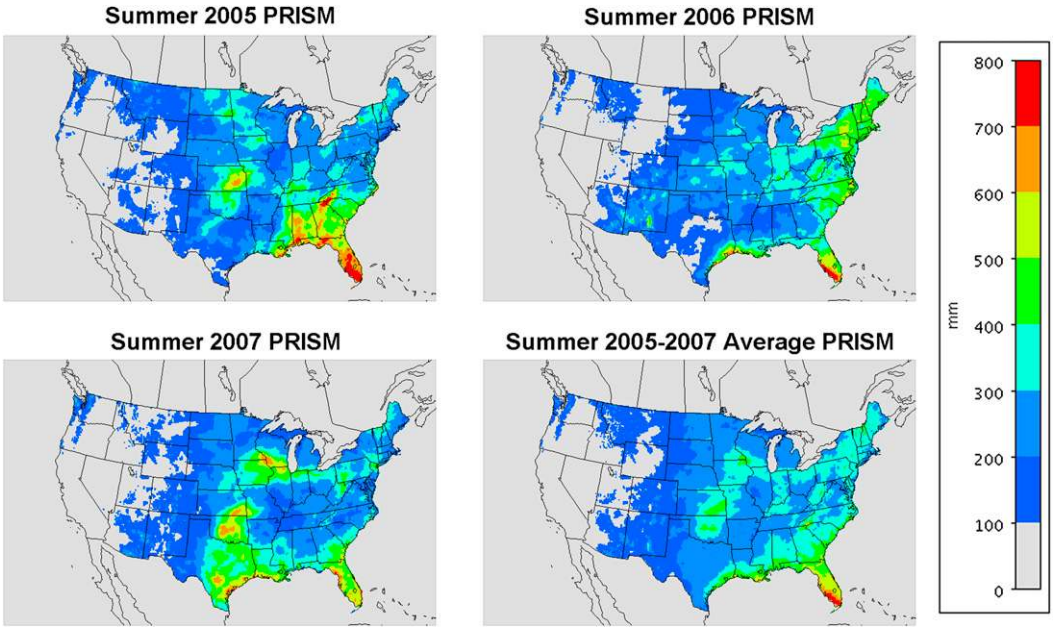

FIG. 4. Summer season total precipitation over the continental United States during each year of the study period and average summer precipitation for the period as represented by PRISM.

similar results. To illustrate this, Fig. 3 shows the average monthly accumulated precipitation analogous to Fig. 2, but now results from simulations using 36-km grid spacing are evaluated against PRISM data. Essentially similar results were found where improvements occur primarily in the warm seasons and the strong positive bias in the base case (case KF) was reduced with the treatment of subgrid cloud–radiation effects (case RadKF) and reduced further with the addition of the new dynamic τ formulation (case RadTauKF).

b. *Effect on summertime precipitation*

Because these modifications had their greatest effect during the summer season when convection is prevalent, we focus on the summer season (June–August) of each year. The patterns of precipitation that actually fell across the continental United States during the summers of 2005–07 vary considerably, as shown in Fig. 4. The PRISM data show that the summer of 2006 was very wet in the Northeast states compared to the other two summers in the study. On the other hand, the Southeast states had the most precipitation during the summer of 2005 and the summer of 2007 was exceptionally dry in that area. In the Great Plains region, the summers of 2005 and 2007 both had a relatively large amount of rainfall, with 2006 being generally much drier. Obviously, these three summers provided a wide variety of conditions with which to test our modifications to the Kain–Fritsch CPS.

Figure 5 shows the average summer precipitation pattern derived from the PRISM data along with the corresponding average summer precipitation simulated by each of the three WRF configurations using 12-km grid spacing. Use of the standard Kain–Fritsch CPS (KF) produced a significant excess of precipitation over almost all of the eastern United States, with the greatest excess in the Southeast region. There are also areas of excess precipitation over the Great Lakes and Midwest regions, and over mountainous areas of Colorado and New Mexico. Accounting for subgrid-scale cloud effects on radiation (RadKF) helped to reduce the excess precipitation in all of these areas, but most areas east of the Mississippi River still show an obvious excess of precipitation. In contrast, the small areas of heavy precipitation (>400 mm) indicated by PRISM over eastern Kansas and central Oklahoma are slightly underrepresented by the RadKF model configuration. With the addition of the dynamic τ formulation (RadTauKF), only the Southeast and mid-Atlantic regions continue to show localized areas of excess precipitation. However, there is now a deficit of precipitation relative to PRISM across much of the central plains region and along the Texas and Louisiana coasts.

Figure 6 shows the fractional decrease in simulated precipitation in June–August (JJA) relative to the standard Kain–Fritsch CPS from only the subgrid-scale radiation treatment and the additional effect of adding the dynamic τ formulation. Some of the model grid cells

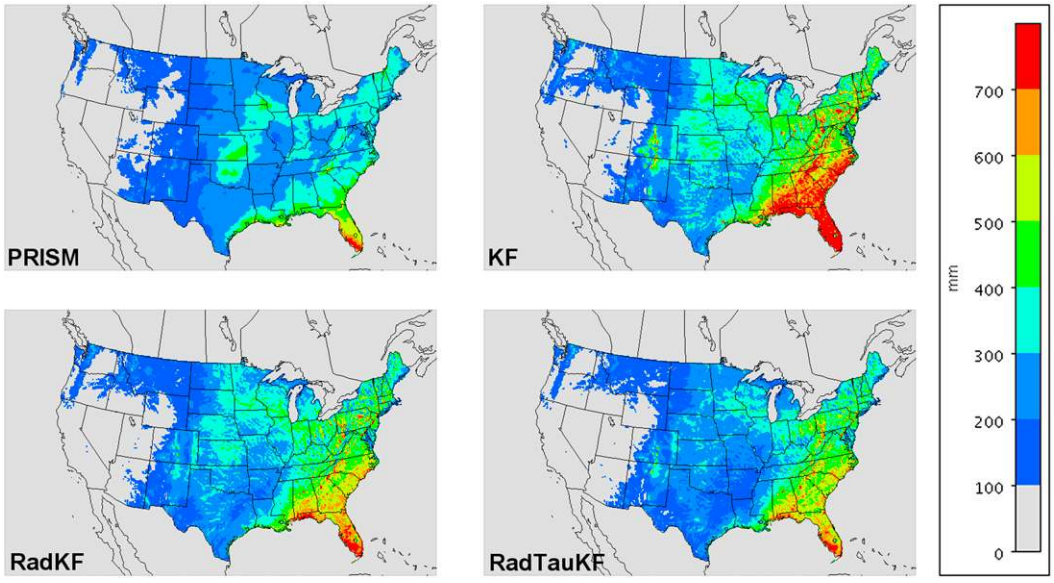

FIG. 5. Average summer precipitation from (top left) PRISM compared to (top right) WRF using the standard Kain–Fritsch CPS (KF), (bottom left) WRF using the subgrid radiation treatment (RadKF), and (bottom right) WRF using both the subgrid radiation treatment and dynamic τ formulation (RadTauKF). All WRF test cases shown here used 12-km grid spacing.

in southern California and the Southwest region show an almost complete elimination of simulated precipitation just from the radiation treatment, and the number of these cells increases with the addition of the dynamic τ formulation. These cells accurately showed little or no summertime precipitation in the standard KF configuration and subsequent modifications resulted in much the same outcome. Calculation of fractional change with a near-zero value for the standard KF in the denominator results in these large (or quasi infinite) reductions. Nonetheless, Fig. 6a clearly shows that reductions in simulated precipitation from the subgrid radiation treatment are more significant in states along the Atlantic Ocean and Gulf of Mexico and in western areas at high elevation. However, the effect of the dynamic τ formulation is more concentrated in the Midwest and Great Plains states. Obviously, there is still an opportunity for further improvement with some areas now having too little summer precipitation and other still having too much, but the subgrid radiation treatment and the dynamic τ formulation are certainly improving the overall precipitation bias across the continental United States (Fig. 2).

Figure 7 shows the monthly mean absolute error (MAE) for each of the three WRF configurations relative to the PRISM precipitation data. With the standard Kain–Fritsch CPS, MAE is 40–45 mm during the summer months. It is interesting to note that the magnitude of this summertime MAE is not much greater than the magnitude of the bias indicated by the plot of the observed and simulated mean monthly precipitation in Fig. 2, suggesting that simulated precipitation is excessive across most if not all of the continental United States. The MAE obtained from

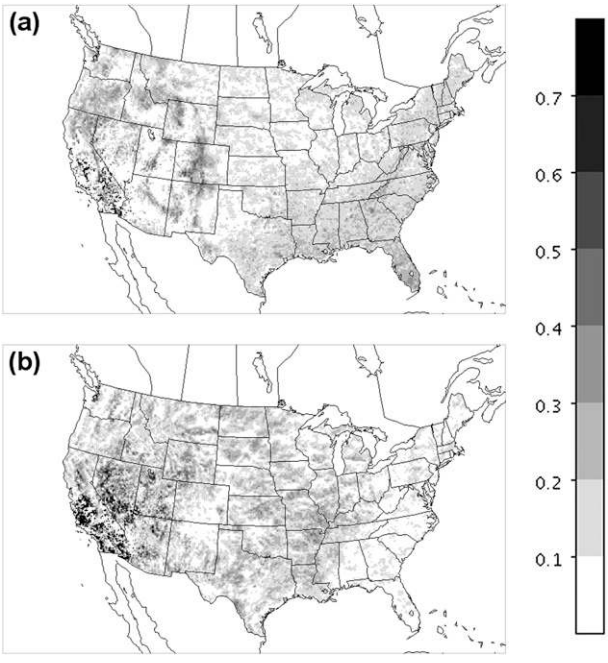

FIG. 6. Fractional decrease in simulated JJA precipitation relative to the standard Kain–Fritsch CPS showing (a) the effect of only the subgrid radiation treatment and (b) the additional effect of adding the dynamic convective time-scale formulation. Results shown here are from test cases using 12-km grid spacing.

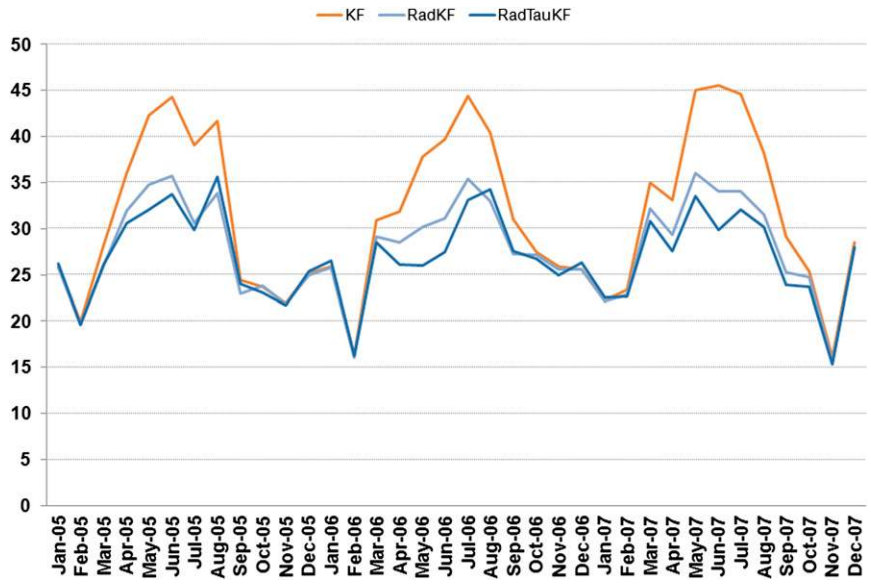

FIG. 7. MAE for WRF test cases using 12-km grid spacing vs PRISM for each month of the study period.

treating subgrid-scale radiation (RadKF) is significantly reduced during the warm months when convective precipitation is common, and addition of the dynamic τ formulation (RadTauKF) reduces MAE further for most of these months. While Fig. 5 does show a few areas where simulated precipitation is deficient relative to PRISM, overall the accuracy is improved with the dynamic τ formulation.

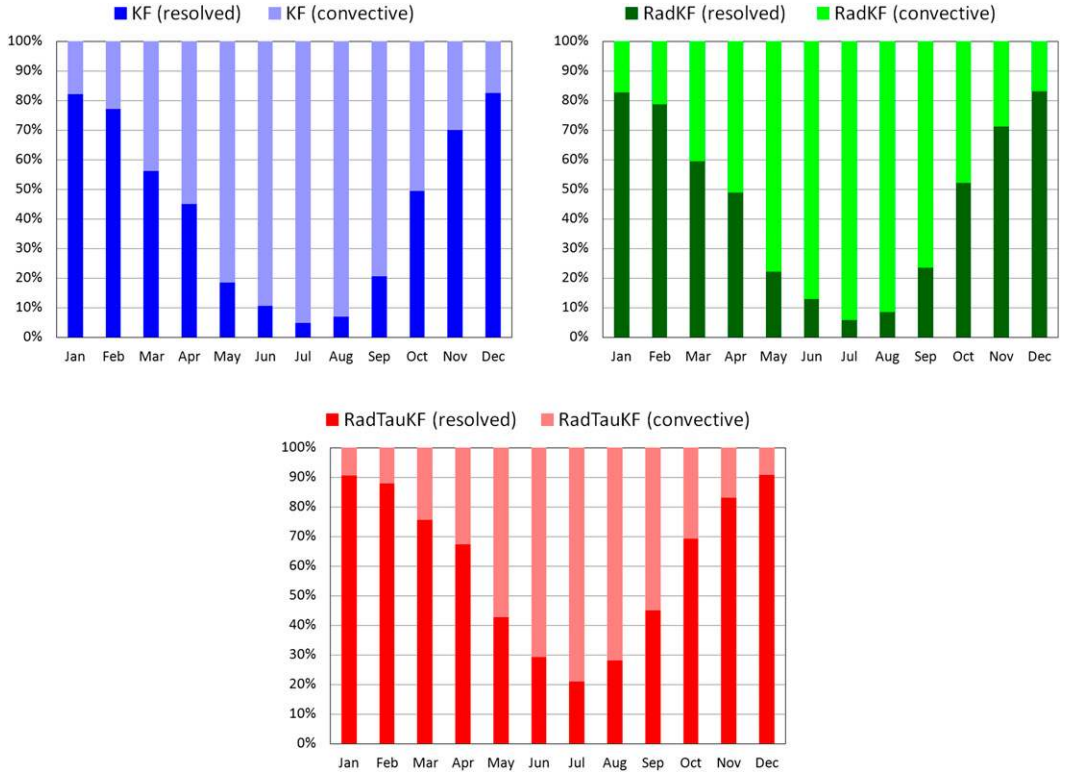

FIG. 8. Resolved and convective proportions of total simulated precipitation with 12-km grid spacing for each month from each of the three test cases during the entire 3-yr simulation period.

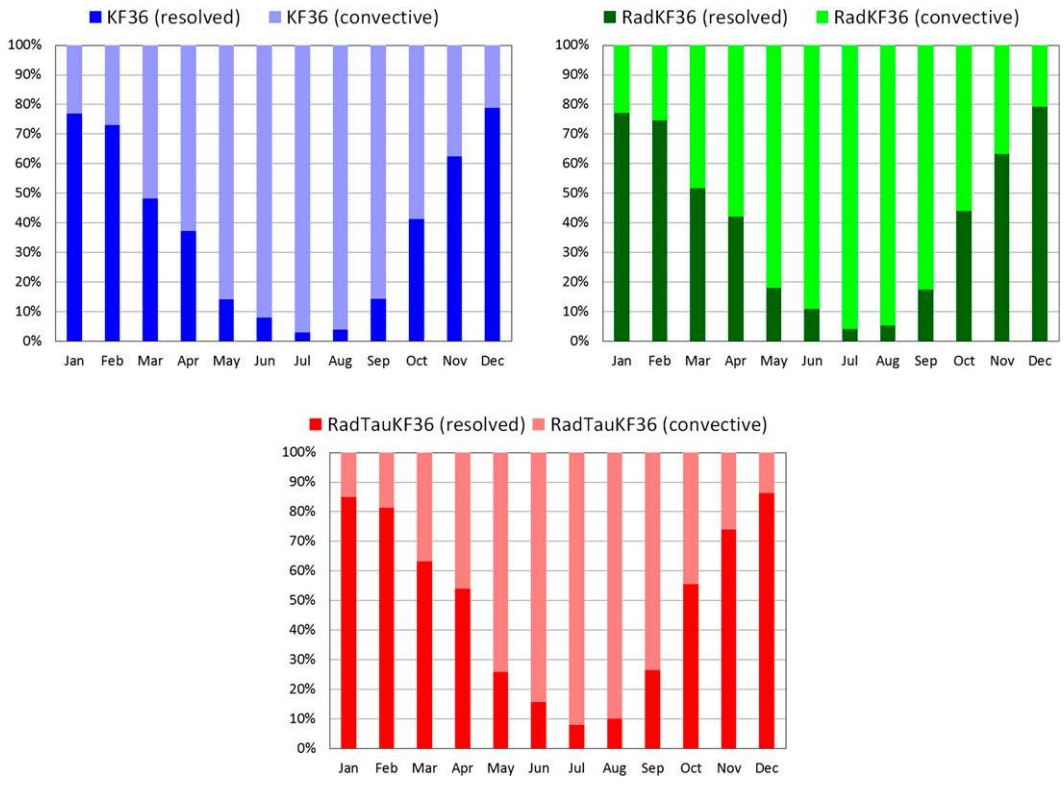

FIG. 9. As in Fig. 8, but for 36-km grid spacing.

c. *Effect on precipitation type (resolved vs convective)*

These modifications also impact the proportion of resolved versus parameterized precipitation, leaving more moisture and convective instability to be acted upon by resolved model processes. Figure 8 shows the average monthly proportion of total simulated precipitation that is produced by grid-scale water vapor saturation (resolved) versus that produced by the convective parameterization (convective). The values shown for each month are derived from all 3 yr of the simulation (2005–07) and from all model grid cells over the continental United States. The effect of adding the subgrid radiation treatment is minimal. However, when the dynamic τ formulation is added, the fraction of resolved precipitation is increased for every month, not just in the warm season. But the increase in resolved precipitation is certainly more significant in the warm months when the convective parameterization is more often applied to address convective instability.

To once again test the robustness of the new dynamic τ formulation, we analyzed the proportions of resolved versus parameterized precipitation from our simulations using 36-km grid spacing. The results in Fig. 9 show similar effects as were found with 12-km grid spacing. The resolved fraction of the total simulated precipitation is somewhat less with 36-km grid spacing, and the effect of the subgrid-scale cloud–radiation treatment is rather small. But the new dynamic τ formulation still results in increased fractions of resolved precipitation, especially during the spring and summer when convective precipitation is dominant.

d. *Effect on other surface weather variables*

Aside from the improvement in overall precipitation bias and error, the dynamic τ formulation could also impact the simulation of other important near-surface variables. To assess its impact, we compared our simulations using 12-km grid spacing to hourly observations of 2-m temperature, 2-m water vapor mixing ratio, and 10-m wind speed data. To assure data quality, we used only standard observation data [Surface Aviation Observation (SAO) and METAR] from the Meteorological Assimilation Data Ingest System (MADIS) data repository provided by the National Oceanic and Atmospheric Administration. These reports provided over 30 000 000 hourly observations across the WRF modeling domain during the 2005–07 simulation period.

TABLE 1. Mean bias for surface meteorological variables simulated with 12-km grid spacing based on comparisons to observations in MADIS.

	KF	RadKF	RadTauKF
	2-m temperature (K)		
2005	−0.0226	−0.0793	−0.0117
2006	0.0396	−0.0034	0.0836
2007	−0.1190	−0.1552	−0.0739
2005–07	−0.0340	−0.0793	−0.0007
	2-m water vapor mixing ratio ($g\,kg^{-1}$)		
2005	0.1956	0.1977	0.1786
2006	0.2885	0.2714	0.2041
2007	0.4842	0.4587	0.4294
2005–07	0.3228	0.3092	0.2707
	10-m wind speed ($m\,s^{-1}$)		
2005	0.1729	0.1438	0.1474
2006	0.2283	0.2005	0.2067
2007	0.2467	0.2193	0.2236
2005–07	0.2160	0.1879	0.1926

TABLE 2. MAEs for surface meteorological variables simulated with 12-km grid spacing based on comparison to observations in MADIS.

	KF	RadKF	RadTauKF
	2-m temperature (K)		
2005	2.1833	2.1630	2.1806
2006	2.1239	2.1059	2.1331
2007	2.1330	2.1154	2.1251
2005–07	2.1467	2.1281	2.1463
	2-m water vapor mixing ratio ($g\,kg^{-1}$)		
2005	1.1388	1.1284	1.1742
2006	1.1464	1.1333	1.1781
2007	1.1418	1.1263	1.1511
2005–07	1.1423	1.1293	1.1678
	10-m wind speed ($m\,s^{-1}$)		
2005	1.4225	1.4196	1.4205
2006	1.4553	1.4520	1.4543
2007	1.4726	1.4698	1.4693
2005–07	1.4501	1.4471	1.4480

Statistical comparisons of simulated and observed weather data were made using standard procedures provided by AMET.

Table 1 shows the resulting analysis of mean bias for each year of the test period and for all years combined. For 2-m temperature, the mean bias from the standard Kain–Fritsch CPS is quite small for each year and only slightly negative at −0.0340 K for the entire test period. The RadKF case shows a minor trend toward more negative bias, with a bias of −0.1552 K for 2007 and a bias of −0.0793 K for the entire period. Interestingly, adding the dynamic τ formulation to the subgrid radiation treatment almost totally eliminates bias for the 3-yr period with a value of −0.0007 K.

For water vapor mixing ratio, WRF was showing a rather strong positive bias in the standard configuration, as in other studies (Bullock et al. 2014; Otte et al. 2012). For 2007, the bias is 0.4842 $g\,kg^{-1}$, and for the entire test period the computed bias is 0.3228 $g\,kg^{-1}$. Adding the subgrid radiation treatment helps to reduce this moist bias slightly to 0.3092 $g\,kg^{-1}$ for the 3-yr period. With the addition of the dynamic τ formulation, we see a larger reduction to 0.2707 $g\,kg^{-1}$ for the 3-yr period, but this bias remains somewhat high. There has been some suspicion that the NCEP–DOE AMIP-II Reanalysis data, to which we nudged these simulations, may have a moist bias and this could be contributing. However, Bullock et al. (2014) found a similar moist bias that was reduced with stronger nudging toward the same NCEP–DOE AMIP-II Reanalysis data. Therefore, we conclude that the cause is internal to the WRF Model itself (and possibly related to the choice of land surface model).

For wind speed, Table 1 shows very little difference in mean bias between the three test simulations. Wind speed is biased slightly high, with annual values and the 3-yr value all hovering around 0.2 $m\,s^{-1}$. From the above results, we conclude that the dynamic τ formulation is certainly not degrading bias in the simulation of basic surface weather conditions and may actually be helping to reduce some biases toward zero.

Table 2 shows a similar analysis for mean absolute error. For these MAE values, all differences between the WRF test simulations are very small. The mean absolute errors for all variables, for each year of the test period and for all years combined, are all the same within two significant digits. For 2-m temperature, mean absolute error is between 2.1 and 2.2 K. For water vapor mixing ratio, it is between 1.1 and 1.2 $g\,kg^{-1}$. For wind speed, the mean absolute error is between 1.4 and 1.5 $m\,s^{-1}$. From these results we conclude that the effect of the dynamic τ formulation on the error in our simulation of surface-level temperature, humidity, and wind is negligible.

e. *Effect on tropical systems*

As mentioned above, Bacmeister et al. (2007) found that use of a larger τ led to marked improvements in hurricane spinup time and intensity in a high-resolution global climate simulation. Given that the hurricane season of 2005 was extremely active for the United States, it presents an opportunity to investigate the effect of our dynamic τ formulation on simulated precipitation from landfalling tropical systems. We first investigated the simulated precipitation pattern at the time of landfall for Hurricane Katrina, one of the most

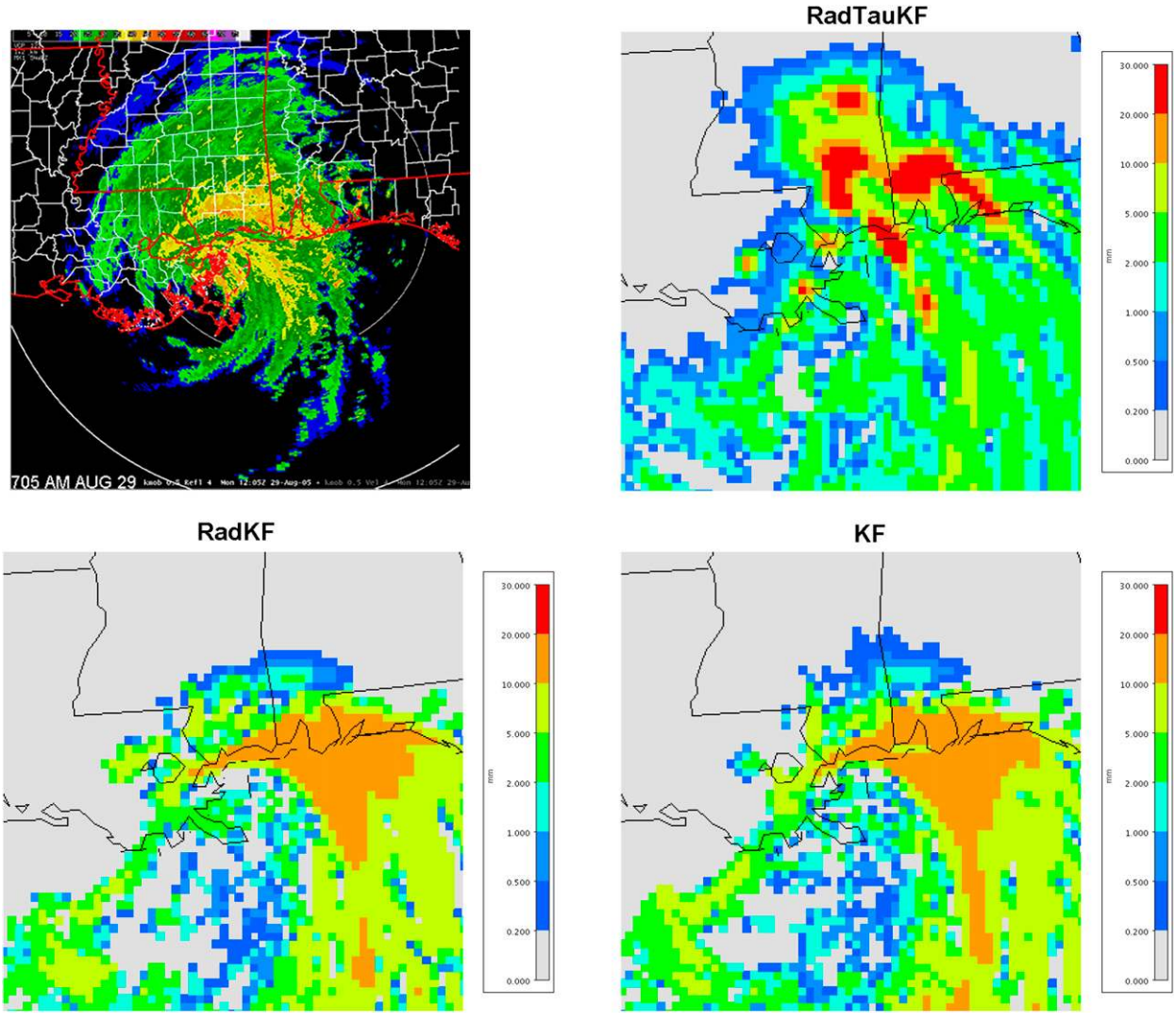

FIG. 10. Comparison of a KMOB radar sweep at 1205 UTC 29 Aug 2005 to simulated precipitation from 1200 to 1300 UTC for each WRF test case using 12-km grid spacing.

devastating hurricanes in the history of the United States. Figure 10 shows the WSR-88D radar reflectivity pattern from Mobile, Alabama (KMOB), at 1205 UTC on 29 August 2005. Also shown in that figure are the simulated 1-h total precipitation patterns as of 1300 UTC from all three WRF test configurations using 12-km grid spacing. While instantaneous radar reflectivity is not directly comparable to hourly accumulated precipitation, this sort of comparison can identify gross pattern discrepancies. The pattern from the standard Kain–Fritsch CPS (KF) and that from the addition of the subgrid radiation treatment (RadKF) are nearly identical and neither shows the extent of inland precipitation that was on going at the time of landfall. However, when the dynamic τ formulation is also added (RadTauKF), the simulation shows a much more realistic pattern of heaviest precipitation inland and to the right of Katrina's position at landfall.

The primary motivation for dynamical downscaling with WRF was to better resolve the effects of future climate change as represented by global climate models. Inland flooding is one of the most lethal aspects of landfalling tropical systems. Therefore, it is important to represent the accumulated precipitation from these high-impact, short-duration events accurately. To better evaluate our test simulations, we obtained hourly precipitation data from the Multisensor Precipitation Estimator (MPE). Figure 11 shows the accumulated precipitation total from 0000 UTC 29 August to 0000 UTC 31 August 2005 from MPE data and the

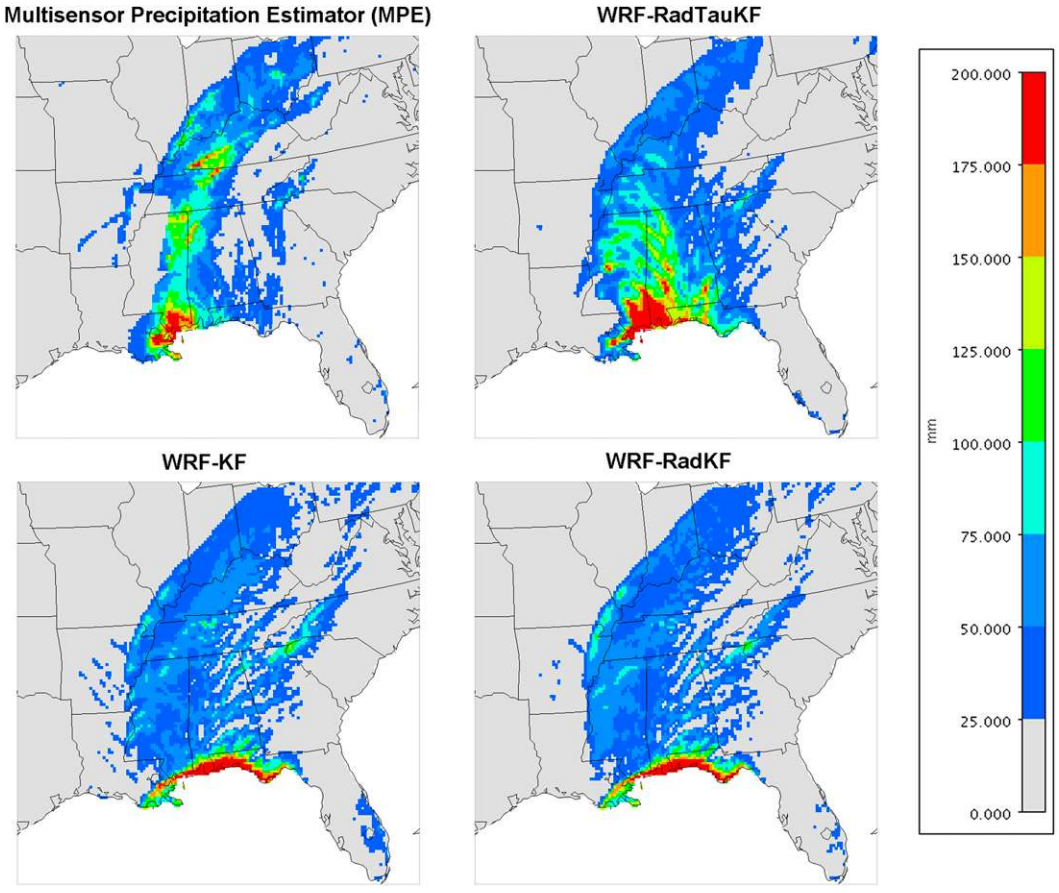

FIG. 11. Accumulated Hurricane Katrina landfall precipitation for the period 0000 UTC 29 Aug–0000 UTC 31 Aug based on the MPE and simulated by each of the WRF test cases using 12-km grid spacing.

corresponding patterns of simulated precipitation from our three test cases using 12-km grid spacing. It should be noted that the MPE was missing data for the lower Mississippi River area during this time period. As with the snapshot of precipitation at landfall, the RadTauKF case shows more precipitation inland of the landfall point and matches the MPE data much better than do the other cases. To confirm this improved representation of Hurricane Katrina was indicative of truly improved skill, we also performed similar analyses for the three other major hurricanes (category 3+) that made landfall in the United States during our study period (all were in 2005).

Figure 12 shows the accumulated precipitation for Hurricane Dennis from 0000 UTC 10 July to 0000 UTC 12 July 2005, as represented by the MPE and the three WRF test cases using 12-km grid spacing. Here again, the case using the dynamic τ formulation shows a much more realistic pattern with heavy precipitation well inland. The other cases once again are very similar and show no heavy precipitation inland with only moderate amounts near the coastline. Figures 13 and 14 show similar analyses for Hurricanes Rita and Wilma, respectively. For Hurricane Rita, the difference in the patterns of simulated precipitation from the RadTauKF case and the other two cases is not quite so striking, but the dynamic τ formulation does provide a more realistic result. For Hurricane Wilma, the RadTauKF case shows maximum precipitation amounts closer to the observed values across central Florida.

Besides differences in the precipitation pattern, we also found the highest simulated 10-m wind speeds from the RadTauKF case (not shown) to be stronger and closer to the center of circulation than for both of the other cases. It appears that by allowing the resolved-scale processes in WRF to produce more of the precipitation and release more latent heat, a more realistic simulation of tropical storm structure is achieved.

4. Summary and conclusions

This work has evaluated the performance of a dynamically based convective adjustment time scale τ for

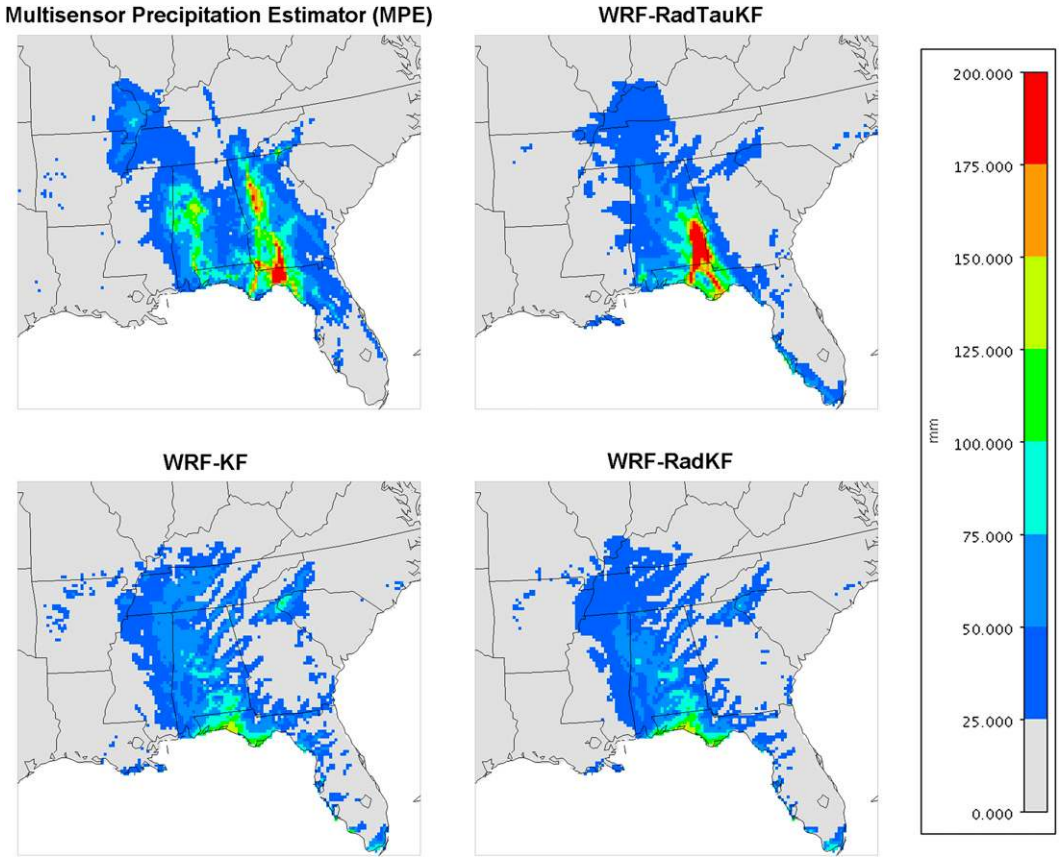

FIG. 12. As in Fig. 11, but for Hurricane Dennis for the period 0000 UTC 10 Jul–0000 UTC 12 Jul.

the dissipation of CAPE in the Kain–Fritsch CPS. This new formulation for τ is linked to the strength of the parameterized updraft, the physical height of the convective cloud, and the time required for convective overturning to stabilize the atmosphere. It is inspired by the work of Bechtold et al. (2008) and Grant and Lock (2004).

This study was motivated to investigate the parameterization of convection due to a positive bias in simulated precipitation that was especially prevalent in the summer months (June–August). Bullock et al. (2014) showed this excess of simulated summertime precipitation became amplified as the model's horizontal grid spacing was reduced from 36 to 12 km, to length scales generally recognized as challenging to all convective parameterization schemes. Alapaty et al. (2012) previously implemented a treatment in WRF to address the effect of subgrid-scale clouds on radiation. This study applied that treatment at 12-km grid spacing and, thus, reduced the positive precipitation bias across the continental United States from 30% to 21% based on comparisons to PRISM data during the entire 3-yr simulation period. In the standard Kain–Fritsch scheme, a shorter time is used for the dissipation of CAPE as model grid spacing is reduced. However, less vigorous parameterized convection should occur when finer resolution is used. When the new dynamic formulation is implemented, a marked increase occurs in the convective time scale across nearly the entire model domain. The new dynamic τ, when used in addition to the subgrid-scale cloud–radiation treatment, further reduced the positive precipitation bias to 15% in our 12-km WRF simulation of 2005–07.

The effects of the subgrid radiation scheme and dynamic τ formulation on summertime precipitation bias were not the same in all locations. Whereas the effect of the subgrid-scale cloud–radiation scheme on reducing simulated precipitation was greater in the eastern and Gulf Coast areas than in the central and northern plains, the dynamic τ formulation brought about a greater reduction in precipitation in the central region relative to the eastern region of the United States. The effects from both modifications were highly varied across the Rocky Mountains and West Coast regions where topography is a stronger driver of convection and where summertime convective precipitation is lighter.

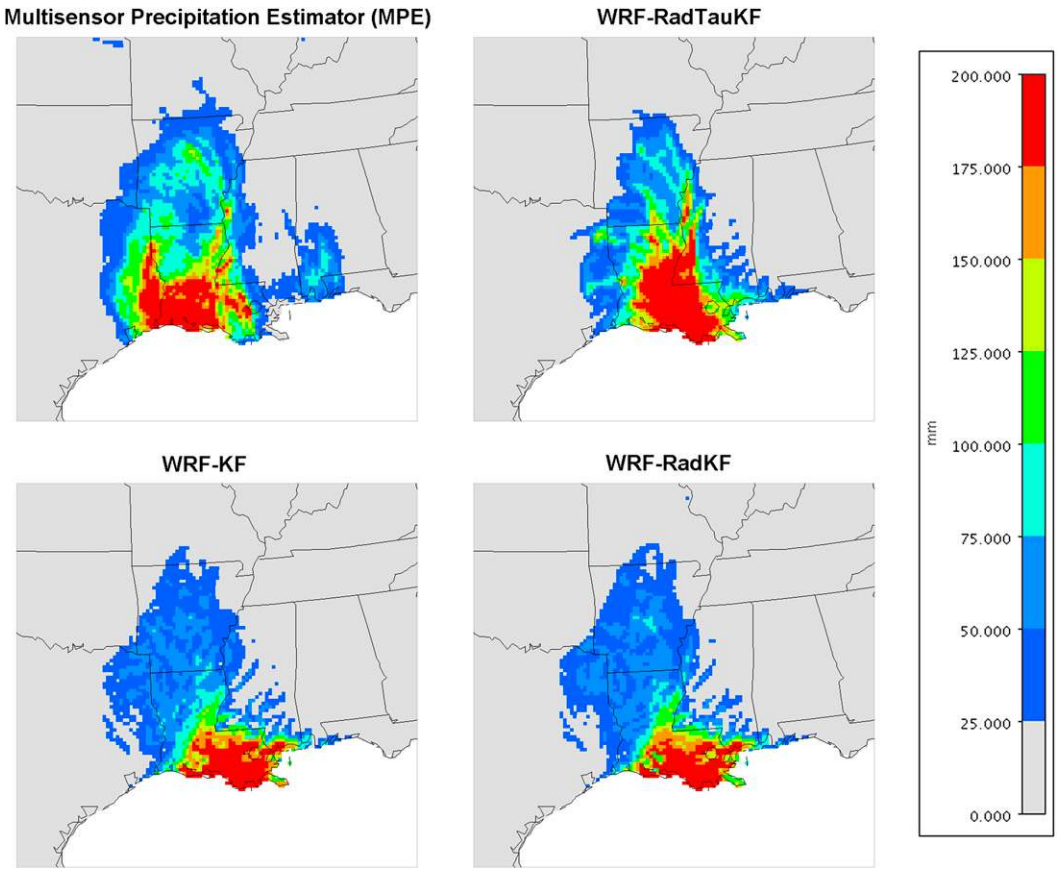

FIG. 13. As in Fig. 11, but for Hurricane Rita for the period 1200 UTC 23 Sep–1200 UTC 25 Sep.

Besides providing an additional reduction to the positive precipitation bias beyond that found from the subgrid radiation scheme alone, the dynamic τ formulation also further reduced the mean absolute error in precipitation across the entire model domain. Of course, both of these modifications had little effect on the winter months when convection is nearly absent across most of North America. But in the other portions of all 3 yr of the simulation, the dynamic τ formulation provided a noticeable improvement in simulated precipitation while also delivering some improvement in the bias of 2-m temperature and water vapor mixing ratio.

One interesting effect that was observed from the dynamic τ formulation that was not evident from the subgrid radiation scheme was the redistribution of simulated precipitation from the convective form to the resolved form. Using longer convective adjustment times in the subgrid parameterization allowed the model-resolved precipitation processes to be more prevalent. While the standard Kain–Fritsch approach, both with and without the subgrid radiation scheme, showed 10% or less of the total precipitation in the resolved form during the summer months, addition of the dynamic τ formulation brought that fraction up to 20%–30%. It appears that this allowance of resolved precipitation processes also had a profound and positive effect on the simulated patterns of inland precipitation during the landfall of tropical storms. Overall, the dynamic τ formulation was found to offer significant improvements in simulated summertime precipitation.

The specific physical dependencies in the τ formulation are difficult to justify quantitatively. There are simply not enough empirical data available for a more robust formula. Also, there are other aspects of the WRF Model configuration that can strongly affect the amount and type of simulated precipitation, such as the cloud microphysics scheme. Nonetheless, these results not only confirm previous studies showing sensitivity to τ, they provide important clues that could lead to a more quantitatively robust formulation. Specifically, they provide evidence to suggest that a parameterized adjustment time scale that depends on CAPE and cloud depth is useful. Undoubtedly, there are other factors involved and more optimal ways of quantifying

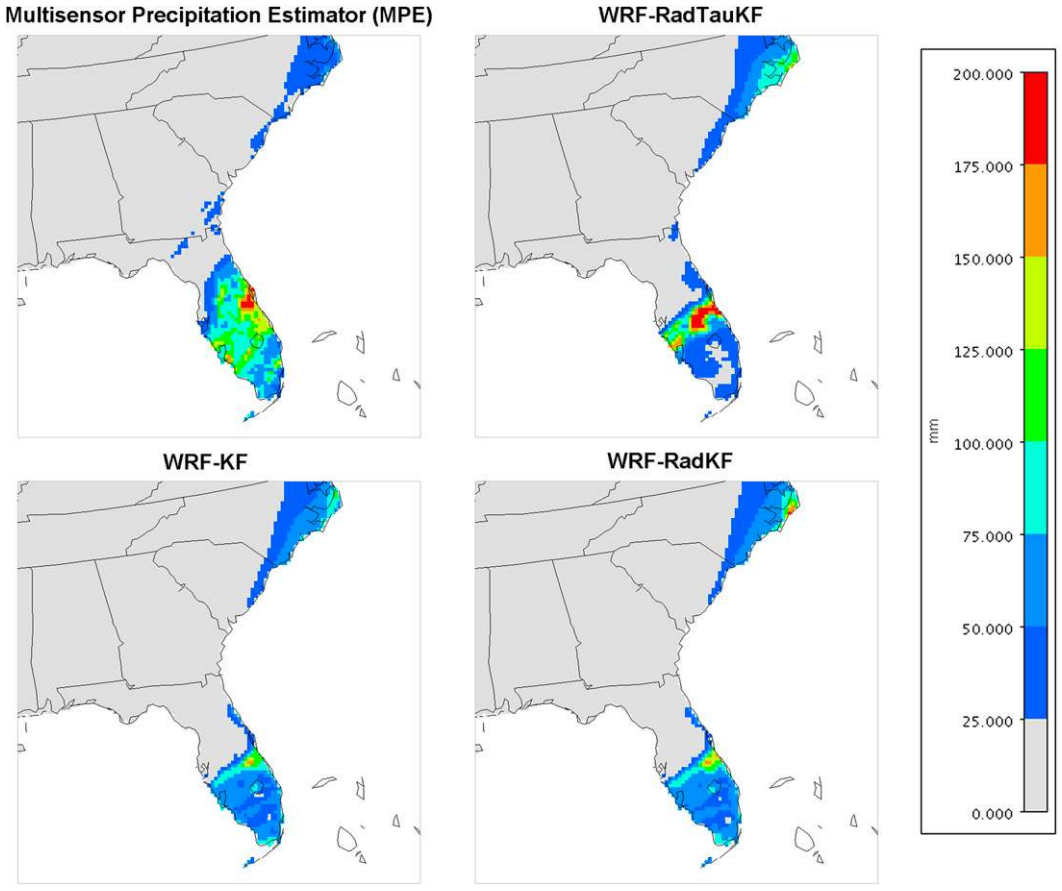

FIG. 14. As in Fig. 11, but for Hurricane Wilma for the period 0000 UTC 24 Oct–0000 UTC 25 Oct.

key relationships. The positive bias in the water vapor mixing ratio we found when comparing model simulations to surface-level measurements remains a concern. Future work should continue to investigate these factors and relationships, perhaps using cloud-resolving models. There is significant potential for further improvements in convective parameterization, particularly for model grid spacing near or below 10 km.

Acknowledgments. The U.S. Environmental Protection Agency through its Office of Research and Development funded and managed the research described here. It has been subjected to agency review and approved for publication. The WRF Model is made available by the National Center for Atmospheric Research, funded by the National Science Foundation. We thank Robert Gilliam at the U.S. EPA for his assistance with the AMET system for evaluation of modeling results. We also thank Megan Mallard, Christopher Nolte, and Tanya Spero at the U.S. EPA for their comments and suggestions for the improvement of this work.

REFERENCES

Alapaty, K., R. V. Madala, and S. Raman, 1994a: Numerical simulation of orographic convective rainfall with Kuo and Betts–Miller cumulus parameterization schemes. *J. Meteor. Soc. Japan,* **72,** 123–137.

——, S. Raman, R. V. Madala, and U. C. Mohanty, 1994b: Monsoon rainfall simulation with the Kuo and Betts–Miller schemes. *Meteor. Atmos. Phys.,* **53,** 33–49, doi:10.1007/BF01031903.

——, J. A. Herwehe, T. L. Otte, C. G. Nolte, O. R. Bullock, M. S. Mallard, J. S. Kain, and J. Dudhia, 2012: Introducing subgrid-scale cloud feedbacks to radiation for regional meteorological and climate modeling. *Geophys. Res. Lett.,* **39,** L24809, doi:10.1029/2012GL054031.

Appel, K. W., R. C. Gilliam, N. Davis, A. Zubrow, and S. C. Howard, 2011: Overview of the Atmospheric Model Evaluation Tool (AMET) v1.1 for evaluating meteorological and air quality models. *Environ. Modell. Software,* **26,** 434–443, doi:10.1016/j.envsoft.2010.09.007.

Arakawa, A., and W. H. Schubert, 1974: Interaction of a cumulus cloud ensemble with the large-scale environment, Part I. *J. Atmos. Sci.,* **31,** 674–701, doi:10.1175/1520-0469(1974)031<0674:IOACCE>2.0.CO;2.

Bacmeister, J., R. Pegion, S. Schubert, M. Suarez, and C. Tassone, 2007: Explicitly resolved mesoscale motions in high resolution

global simulations. *Geophysical Research Abstracts,* Vol. 9, Abstract 04600. [Available online at http://meetings.copernicus.org/www.cosis.net/abstracts/EGU2007/04600/EGU2007-J-04600.pdf.]

Bechtold, P., M. Köhler, T. Jung, F. Doblas-Reyes, M. Leutbecher, M. J. Rodwell, F. Vitart, and G. Balsamo, 2008: Advances in simulating atmospheric variability with the ECMWF model: From synoptic to decadal time-scales. *Quart. J. Roy. Meteor. Soc.,* **134,** 1337–1351, doi:10.1002/qj.289.

Betts, A. K., 1986: A new convective adjustment scheme. Part I: Observational and theoretical basis. *Quart. J. Roy. Meteor. Soc.,* **112,** 677–691, doi:10.1002/qj.49711247307.

Bowden, J. H., T. L. Otte, C. G. Nolte, and M. J. Otte, 2012: Examining interior grid nudging techniques using two-way nesting in the WRF Model for regional climate modeling. *J. Climate,* **25,** 2805–2823, doi:10.1175/JCLI-D-11-00167.1.

——, C. G. Nolte, and T. L. Otte, 2013: Simulating the impact of the large-scale circulation on the 2-m temperature and precipitation climatology. *Climate Dyn.,* **40,** 1903–1920, doi:10.1007/s00382-012-1440-y.

Bullock, O. R., Jr., K. Alapaty, J. A. Herwehe, M. S. Mallard, T. L. Otte, R. C. Gilliam, and C. G. Nolte, 2014: An observation-based investigation of nudging in WRF for downscaling surface climate information to 12-km grid spacing. *J. Appl. Meteor. Climatol.,* **53,** 20–33, doi:10.1175/JAMC-D-13-030.1.

Chen, F., and J. Dudhia, 2001: Coupling an advanced land surface–hydrology model with the Penn State–NCAR MM5 modeling system. Part I: Model implementation and sensitivity. *Mon. Wea. Rev.,* **129,** 569–585, doi:10.1175/1520-0493(2001)129<0569:CAALSH>2.0.CO;2.

Collins, W. D., and Coauthors, 2006: The formulation and atmospheric simulation of the Community Atmosphere Model version 3 (CAM3). *J. Climate,* **19,** 2144–2161, doi:10.1175/JCLI3760.1.

Daly, C., R. P. Neilson, and D. L. Phillips, 1994: A statistical–topographic model for mapping climatological precipitation over mountainous terrain. *J. Appl. Meteor.,* **33,** 140–158, doi:10.1175/1520-0450(1994)033<0140:ASTMFM>2.0.CO;2.

Done, J. M., G. C. Craig, S. L. Gray, P. A. Clark, and M. E. B. Gray, 2006: Mesoscale simulations of organized convection: Importance of convective equilibrium. *Quart. J. Roy. Meteor. Soc.,* **132,** 737–756, doi:10.1256/qj.04.84.

Emanuel, K. A., and K. Bister, 1996: Moist convective velocity scales. *J. Atmos. Sci.,* **53,** 3276–3285, doi:10.1175/1520-0469(1996)053<3276:MCVABS>2.0.CO;2.

——, J. D. Neelin, and C. S. Bretherton, 1994: On large-scale circulations in convecting atmospheres. *Quart. J. Roy. Meteor. Soc.,* **120,** 1111–1143, doi:10.1002/qj.49712051902.

Frank, W. M., 1983: The cumulus parameterization problem. *Mon. Wea. Rev.,* **111,** 1859–1871, doi:10.1175/1520-0493(1983)111<1859:TCPP>2.0.CO;2.

——, and C. Cohen, 1987: Simulation of tropical convective systems. Part I: A cumulus parameterization. *J. Atmos. Sci.,* **44,** 3787–3799, doi:10.1175/1520-0469(1987)044<3787:SOTCSP>2.0.CO;2.

Fritsch, J. M., and C. F. Chappell, 1980: Numerical prediction of convectively driven mesoscale pressure systems. Part I: Convective parameterization. *J. Atmos. Sci.,* **37,** 1722–1733, doi:10.1175/1520-0469(1980)037<1722:NPOCDM>2.0.CO;2.

Grant, A. L. M., and A. P. Lock, 2004: The turbulent kinetic energy budget for shallow cumulus convection. *Quart. J. Roy. Meteor. Soc.,* **130,** 401–422, doi:10.1256/qj.03.50.

Herwehe, J. A., K. Alapaty, T. L. Spero, and C. G. Nolte, 2014: Increasing the credibility of regional climate simulations by introducing subgrid-scale cloud-radiation interactions. *J. Geophys. Res. Atmos.,* **119,** 5317–5330, doi:10.1002/2014JD021504.

Holland, J. Z., and E. M. Rasmusson, 1973: Measurement of atmospheric mass, energy, and momentum budgets over a 500-kilometer square of tropical ocean. *Mon. Wea. Rev.,* **101,** 44–55, doi:10.1175/1520-0493(1973)101<0044:MOTAME>2.3.CO;2.

Hong, S.-Y., and J.-O. J. Lim, 2006: The WRF single-moment 6-class microphysics scheme (WSM6). *J. Korean Meteor. Soc.,* **42,** 129–151.

——, Y. Noh, and J. Dudhia, 2006: A new vertical diffusion package with an explicit treatment of entrainment processes. *Mon. Wea. Rev.,* **134,** 2318–2341, doi:10.1175/MWR3199.1.

Kain, J. S., 2004: The Kain–Fritsch convective parameterization: An update. *J. Appl. Meteor.,* **43,** 170–181, doi:10.1175/1520-0450(2004)043<0170:TKCPAU>2.0.CO;2.

——, and J. M. Fritsch, 1993: Convective parameterization for mesoscale models: The Kain– Fritsch scheme. *The Representation of Cumulus Convection in Numerical Models, Meteor. Monogr.,* No. 46, Amer. Meteor. Soc., 165–170.

Kanamitsu, M., W. Ebisuzaki, J. Woollen, S.-K. Yang, J. J. Hnilo, M. Fiorino, and G. L. Potter, 2002: NCEP–DOE AMIP-II Reanalysis (R-2). *Bull. Amer. Meteor. Soc.,* **83,** 1631–1643, doi:10.1175/BAMS-83-11-1631.

Kuo, H.-L., 1974: Further studies of the parameterization of the influence of cumulus convection on large-scale flow. *J. Atmos. Sci.,* **31,** 1232–1240, doi:10.1175/1520-0469(1974)031<1232:FSOTPO>2.0.CO;2.

Lin, X., D. A. Randall, and L. D. Fowler, 2000: Diurnal variability of the hydrologic cycle and radiative fluxes: Comparisons between observations and a GCM. *J. Climate,* **13,** 4159–4179, doi:10.1175/1520-0442(2000)013<4159:DVOTHC>2.0.CO;2.

Liu, P., B. Wang, and G. A. Meehl, 2007: Sensitivity of MJO to the CAPE lapse time in the NCAR CAM3. *12th Annual CCSM Workshop,* Breckenridge, CO, NSF–DOE.

Lucas, D. D., and Coauthors, 2010: The climate uncertainty quantification project at Lawrence Livermore National Laboratory: I. Initial analysis of the sensitivities and uncertainties in the Community Atmosphere Model. *2010 Fall Meeting,* San Francisco, CA, Amer. Geophys. Union, Abstract GC23F-0981.

Manabe, S., J. Smagorinsky, and R. F. Strickler, 1965: Simulated climatology of a general circulation model with a hydrological cycle. *Mon. Wea. Rev.,* **93,** 769–798, doi:10.1175/1520-0493(1965)093<0769:SCOAGC>2.3.CO;2.

Otte, T., C. Nolte, M. Otte, and J. Bowden, 2012: Does nudging squelch the extremes in regional climate modeling? *J. Climate,* **25,** 7046–7066, doi:10.1175/JCLI-D-12-00048.1.

Skamarock, W. C., and Coauthors, 2008: A description of the Advanced Research WRF version 3. NCAR Tech. Note NCAR/TN–475+STR, 113 pp. [Available online at http://nldr.library.ucar.edu/repository/assets/technotes/TECH-NOTE-000-000-000-855.pdf.]

Stauffer, D. R., and N. L. Seaman, 1994: Multiscale four-dimensional data assimilation. *J. Appl. Meteor.,* **33,** 416–434, doi:10.1175/1520-0450(1994)033<0416:MFDDA>2.0.CO;2.

Wilcox, E. M., and L. J. Donner, 2007: The frequency of extreme rain events in satellite rain-rate estimates and an atmospheric general circulation model. *J. Climate,* **20,** 53–69, doi:10.1175/JCLI3987.1.

Zhang, G. J., and N. A. McFarlane, 1995: Sensitivity of climate simulations to the parameterization of cumulus convection in the Canadian Climate Centre general circulation model. *Atmos.–Ocean,* **33,** 407–446, doi:10.1080/07055900.1995.9649539.